

Insights into Editing from an Ile-tRNA Synthetase Structure with tRNA^{Ile} and Mupirocin

Laura F. Silvan,^{1,3*} Jimin Wang,¹ Thomas A. Steitz^{1,2,3}

Isoleucyl-transfer RNA (tRNA) synthetase (IleRS) joins Ile to tRNA^{Ile} at its synthetic active site and hydrolyzes incorrectly acylated amino acids at its editing active site. The 2.2 angstrom resolution crystal structure of *Staphylococcus aureus* IleRS complexed with tRNA^{Ile} and Mupirocin shows the acceptor strand of the tRNA^{Ile} in the continuously stacked, A-form conformation with the 3' terminal nucleotide in the editing active site. To position the 3' terminus in the synthetic active site, the acceptor strand must adopt the hairpinned conformation seen in tRNA^{Gln} complexed with its synthetase. The amino acid editing activity of the IleRS may result from the incorrect products shuttling between the synthetic and editing active sites, which is reminiscent of the editing mechanism of DNA polymerases.

The aminoacyl-tRNA synthetases that aminoacylate tRNAs with Ile, Thr, and Ala must discriminate against the amino acid containing one less methyl group. Based on thermodynamic considerations, Pauling (1) estimated that isoleucyl-tRNA synthetase (IleRS) could distinguish between Ile and Val by only a factor of 5; however, fewer than 1 error in 3000 occurs (2). To obtain the observed specificity of IleRS, a proofreading activity that hydrolyzes incorrect product is involved (3). It has been proposed (4) that selectivity is achieved by a "double-sieve" mechanism in which amino acids larger than the correct one are sterically excluded at the synthetic active site; in contrast, only smaller amino acids are sterically allowed to bind at a hydrolytic editing active site. The editing and synthetic active sites reside on separate domains (5). In *Thermus thermophilus* apo-IleRS, they are separated by 34 Å and have different specificities for amino acid binding (6).

We address here how amino acid editing is achieved by an active site that is 34 Å distant from the site where the incorrect product is formed and why editing of either the aminoacyl adenylate or the aminoacyl-tRNA requires tRNA^{Ile} (7). One possibility is that the active sites might be brought closer together by a rotation of the editing domain upon addition of tRNA to form a closed cavity that contains the tRNA 3' terminus and both active sites (8). However, the crystal structure of *S. aureus* IleRS complexed with tRNA^{Ile} and Mupirocin presented here suggests an alternative

mechanism involving a tRNA-dependent shuttling of the incorrect product between the two active sites.

The determination of the tRNA-IleRS struc-

ture is summarized in Table 1. The IleRS structure can be divided into three regions of differing function (Fig. 1A). The region that recognizes an unusual anticodon loop conformation is formed by three domains at the COOH-terminus and one at the extreme NH₂-terminus. The dinucleotide (or Rossmann) fold domain forms the core that both activates and transfers the amino acid. The editing domain (connective peptide 1, or CP1) removes any incorrectly incorporated amino acid. tRNA^{Ile} binds along the long axis of the cigar-shaped IleRS structure. An antiparallel pair of α helices binds the minor groove of the tRNA acceptor stem; however, nucleotides in the D-loop of tRNA^{Ile} that were reported to be important for editing (7) do not interact directly with monomeric IleRS. Interactions between IleRS and tRNA^{Ile} that specify recognition of the tRNA^{Ile} sequence, as well as interactions with Mupirocin, are discussed elsewhere (9).

The synthetic and editing active sites are located at the bottoms of two deep clefts and are separated by 34 Å. To mark the synthetic active site we positioned a sulfamyl analogue of glu-

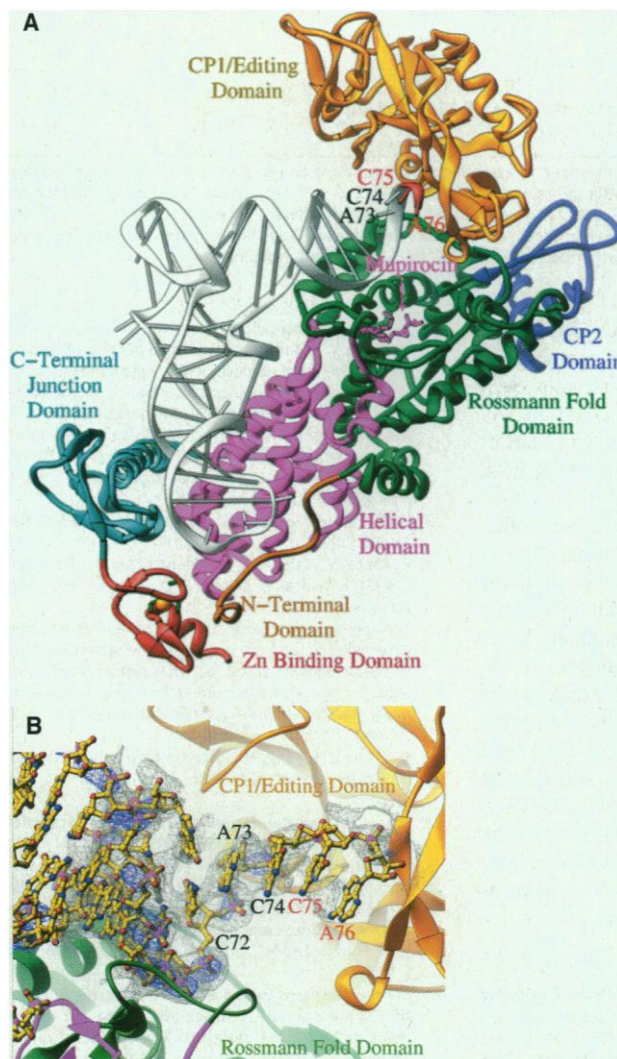


Fig. 1. (A) Structure of the isoleucyl-tRNA synthetase complex with tRNA^{Ile} and Mupirocin. The ordered portion of the tRNA is shown in gold and the two modeled nucleotides are in silver. The Mupirocin drug is in pink. The protein is colored by domain or by section: NH₂-terminal region (orange), Rossmann fold (green), editing domain or CP1 (yellow), acceptor stem binding domain (gray), CP2 domain (blue), helical domain (pink), COOH-terminal junction (turquoise), and Zn-binding domain (red). (B) Experimental electron density for the 3' end of the tRNA^{Ile}. Good density specifies the positions of Ade⁷³ (A73) and Cyt⁷⁴ (C74), but little density exists for the Cyt⁷⁵ (C75) and Ade⁷⁶ (A76) nucleotides, which are model-built to extend the A-form conformation.

¹Departments of Molecular Biophysics and Biochemistry and ²Chemistry, Yale University, and ³Howard Hughes Medical Institute, New Haven, CT 06520-8114, USA.

*Present address: Department of Biological Chemistry and Molecular Pharmacology, Harvard Medical School, 240 Longwood Avenue, Boston, MA 02115, USA.

taminyl adenylate (QSI) from the structure of the glutamyl-tRNA synthetase (GlnRS) ternary complex (10) into the IleRS structure (11); to accomplish this, we superimposed 114 α -carbon atoms in the Rossmann fold domains of the two enzymes with a root-mean-square deviation (rmsd) of 1.3 Å. The binding sites of Mupirocin and the imported adenylate analogue overlap (9). In the previously determined, ligand-free IleRS structure (6), the editing domain binds Val, and the active site region is identified by Tyr³⁹² and His³⁹⁴, whose mutation alters the specificity of the editing activity (12). In this ternary structure, however, one wall of the editing active site cleft showed well-defined electron density, where-

as electron density for the second wall was weak, which suggests some disorder.

The 3' terminus of the tRNA^{Ile} acceptor stem is continuously stacked A-form RNA and is visible in the experimental electron density map to residue Cyt⁷⁴ (Fig. 1B). We have modeled the last two disordered nucleotides to extend the acceptor strand as a continuously stacked helix, which positions the 3' Ade directly into the editing active site. This extended, stacked conformation has previously been observed in the crystal structure of uncomplexed yeast tRNA^{Phe} (13) as well as the structures of tRNAs complexed with class II synthetases (Fig. 2A). Moreover, given the observed positions of Ade⁷³ and Cyt⁷⁴, it is not possible to

model build the 3' end of the tRNA^{Ile} to place the 3' terminus in the synthetic active site. By building the two tRNA 3' terminal nucleotides as A-form RNA, the ribose of Ade⁷⁶ abuts His³⁹² and Tyr³⁹⁴, residues that have been directly implicated in the editing specificity (12) (Fig. 1B). Thus, the complex crystallized here appears to resemble an "editing complex" instead of the "transfer complex" observed in the structure of GlnRS complexed with tRNA^{Gln} and QSI or ATP (10, 14).

Comparison of the structures of the IleRS and GlnRS complexes shows that aminoacylation of tRNA^{Ile} requires that its 3' end adopt the alternative, hairpinned conformation found for tRNA^{Gln} (10, 14). To build a model of a tRNA^{Ile} conformation that would allow aminoacylation, we superimposed (15) 12 backbone phosphates of the tRNA^{Gln} acceptor stem on the equivalent region of tRNA^{Ile}, which gave an rmsd of 1.2 Å (Fig. 2A) and adjusted the phosphate backbone of nucleotides 73 to 76 to avoid steric clashes with the IleRS enzyme (Fig. 2B). In this hairpinned conformation, the bulged Cyt⁷⁴ fits into a small crevice in the surface of the enzyme and the phosphate backbone is near several basic residues. Most notable among these putative interactions is one between the phosphate of Cyt⁷⁵ and Arg⁴⁵⁵ of the Trp-Cys-Ile-Ser-Arg sequence, which is conserved among all synthetases of this class I subclass (16). The hairpinned conformation of the tRNA^{Ile} terminus is likely to differ from that of tRNA^{Gln} because the Gua⁷³ of tRNA^{Gln} makes a sequence-specific contact with a backbone phosphate that cannot be made by the Ade⁷³ of tRNA^{Ile}. Nevertheless, an analogous hairpinned conformation of the acceptor strand is both necessary and feasible when its 3' terminus is being aminoacylated.

In addition, the conformation of the conserved Lys-Met-Ser-Lys-Ser (KMSKS) peptide differs between the GlnRS and IleRS complexes in a manner that may be important for editing. In the GlnRS complex, the Lys of the Val-Met-Ser-Lys-Ser sequence (Lys²⁷⁰) binds the α -phosphate of bound adenosine triphosphate (ATP), presumably to assist in catalysis (14). In the IleRS complex, the equivalent Lys⁵⁹⁸ is more than 15 Å away from the α -phosphate of the model-built aminoacyl-adenylate analogue and instead binds to the carboxylate tail of the inhibitor Mupirocin. Perhaps more significantly for editing, the backbone amide of Lys⁵⁹⁵ of the K⁵⁹⁵MMSKS sequence, as well as the backbone carbonyl of Gly⁵⁹³, binds to the tRNA backbone, thereby stabilizing the extended tRNA conformation and producing an open active site. Because this conserved sequence is in a different orientation in the ligand-free structure of IleRS (6), the conformational change is induced by the binding of tRNA and may be related to the tRNA dependence of editing.

Table 1. Crystallographic data and structure refinement statistics. The IleRS from *S. aureus* (24) was overexpressed, purified, and cocrystallized (25) with *E. coli* tRNA^{Ile}, synthesized in vitro, and Mupirocin, which is an inhibitor. The nucleotides important for specifying tRNA^{Ile} identity (26) are identical in the *E. coli* and the *S. aureus* sequences of tRNA^{Ile}. Crystals were in space group P2₁2₁2₁, diffracted to 2.2 Å resolution, and exhibited two unit cell sizes: a small cell ($a = 70$ Å, $b = 100$ Å, $c = 180$ Å), which formed in the presence of mercury ion, and a large cell ($a = 70$ Å, $b = 100$ Å, $c = 186$ Å). The structure was solved with a combination of multiple wavelength anomalous dispersion (MAD) and multiple isomorphous replacement (MIR) (27). The 18 selenium sites per asymmetric unit were located with the program Solve (28) on MAD data that had been locally scaled with MADPRB (29). Refinement in crystallographic and NMR system (30) with a maximum-likelihood Hendrickson-Lattman (MLHL) target yielded an overall R_{free} value of 28.1% for reflections between 10 and 2.2 Å from the large cell crystal form and an overall R_{free} value of 34.3% for reflections between 10 and 2.9 Å from the small-cell crystal form (27). Native data were collected at Cornell High Energy Synchrotron Source A1 beamline and at a CuK α source; four-wavelength MAD data were collected at Brookhaven National Laboratory (BNL) light source X12C, X4A, and X8C and beamlines at a CuK α source; Dy derivative data were collected at BNL X12C; and Pt derivative data were collected at home CuK α . Large unit cell Hg derivatives were prepared by soaking crystals in 0.1 mM HgI₄ for 12 hours; small unit cell Hg derivatives were prepared by soaking crystals in 1 mM HgI₄ or 0.1 mM HgCl₂ for 12 hours. The small unit cell crystals of selenomethionine-incorporated complexes were created by soaking large unit cell crystals in 0.1 mM HgCl₂ overnight. Pt derivatives were prepared by soaking crystals in 0.1 mM cis-Pt(NH₃)₂Cl₂ for 12 hours. Dy derivatives were prepared by soaking crystals in a stabilization solution 10% saturated with DyCl₃ for 2 hours. $R_{\text{sym}} = \sum |I - \langle I \rangle| / \sum I$, where I is the measurement of intensity. Figure of merit = $\cos(\Delta\phi)$. Phasing power = $[\sum |F_{\text{PH}}(\text{calc})|^2 / \sum |F_{\text{PH}}(\text{obs}) - F_{\text{P}}(\text{calc})|^2]^{1/2}$, where F_{PH} and F_{P} refer to structure factors of derivatives and native data. $R = \sum |F_{\text{obs}} - F_{\text{calc}}| / \sum F_{\text{obs}}$ for all reflections and R_{free} is the R value for 5% of the reflections that were excluded in refinement, where F_{obs} is the observed best native amplitude and F_{calc} is the calculated one from atomic models.

Unit cell dimensions (Å)	70 × 100 × 186	70 × 100 × 180
Native data		
Resolution (Å)	2.2	2.9
Wavelength (Å)	0.94	1.009
Unique reflections	67,758	23,256
Completion (%)	89	90
R_{sym} (%)	7.9	9.9
Derivative data		
Four-wavelength Se resolutions (Å)	2.7–3.0	3.1–3.8
Four-wavelength Se R_{sym} (%)	11.5–13.2	12.5–16.0
Four-wavelength Hg resolutions (Å)	2.8–3.0	2.9–4.0
Four-wavelength Hg R_{sym} (%)	12.1–17.0	8.8–11.8
Pt derivative resolution (Å)	4.0	
Pt derivative R_{sym} (%)	9.4	
Dy derivative resolutions (Å)	3.0–3.5	
Dy derivative R_{sym} (%)	13.4–18.1	
Overall figure of merit (20–4.0 Å)	0.47	0.57
Refinement statistics		
Resolution range (Å)	10–2.2	10–2.9
No. of reflections (>2 σ)	50,930	17,044
No. of atoms (protein/tRNA)	9010	8715
No. of atoms (Mupirocin)	35	35
No. of atoms (Zn/Mg/K)	13	1
No. of atoms (water)	315	169
rmsd bond length (Å)	0.007	0.008
rmsd bond angle (°)	1.4	1.4
R (%)	23.9	22.9
R_{free} (%)	28.1	34.3



Fig. 2. (A) Superposition of the acceptor stems of complexed tRNA^{Ile} (gray thick line), complexed tRNA^{Gln} (black thin line), and uncomplexed tRNA^{Phe} (light thick line). The acceptor strand of tRNA^{Ile} is similar to the continuously stacked conformation of tRNA^{Phe} but differs from the hairpinned conformation of tRNA^{Gln}. (B) and (C) Superposition of tRNA^{Gln} on tRNA^{Ile} on a solvent contact surface representation of IleRS. The acceptor strand of tRNA^{Ile}, represented as a ribbon, is observed at the editing active site. Homology modeling of the tRNA^{Gln} hairpin conformation (ball and stick representation) places its 3' terminus in the synthetic active site 34 Å away. Two orientations are shown to display the active site pockets and the cleft running between them.

The editing domain could hydrolyze a mis-activated or misacylated substrate in one of two different ways: either the editing catalytic site could move to within a few angstroms of the acyl bond of the erroneously acylated substrates or the substrate could shuttle between the two active sites. We suggest that the former possibility is sterically precluded, whereas the second is structurally and kinetically plausible. The fundamental problem with bringing the synthetic and editing active sites together to act on substrate bound to one site is the virtual impossibility of getting the catalytic sites close enough to each other, as they both lie on the bottom of separate clefts. Furthermore, the chemistry of the two reactions requires that the catalytic sites approach the substrate from the same side. Hence, the misacylated substrate must dissociate from the synthetic site and move to the editing site.

The editing mechanism of the IleRS may involve a competition between the two active sites for the same substrate (see Fig. 4). Ed-

iting of the misacylated tRNA may utilize the two known conformations for the 3' end of tRNA: one, the hairpinned conformation seen in the GlnRS complex with tRNA^{Gln}, places the Ade⁷⁶ in the synthetic active site, and the other, the continuously stacked conformation seen in uncomplexed yeast tRNA^{Phe}, places Ade⁷⁶ in the editing active site. If the rate of transfer of the aminoacylated Ade⁷⁶ between the two active sites is faster than the dissociation of the tRNA, then a shuttling mechanism for the misacylated tRNA is possible.

Editing of a valyl-adenylate by a shuttling mechanism requires a rate of its dissociation from the synthetic active site that is fast relative to the rate of amino acid transfer. Further, the rate of adenylate dissociation or the rate of its hydrolysis must be increased by the binding of tRNA^{Ile} (7) to explain the dependence of valyl-adenylate editing on the binding of tRNA^{Ile}. Perhaps tRNA binding facilitates valyl-adenylate dissociation by shifting the KMSKS loop away from the adenylate, thereby increasing its

dissociation rate. Additionally, the IleRS structure in the absence of ligands shows the editing domain overlapping the tRNA binding site (6), whereas the IleRS complex described here shows that the editing domain rotates by about 47° relative to the rest of the molecule, presumably in response to interactions with the tRNA (Fig. 3). In the tRNA complex a deep channel spans the two active sites (Fig. 3A), whereas a ridge lies between the active sites in the unliganded enzyme structure (Fig. 3B).

The editing of either the misacylated tRNA or adenylate depends on nucleotides in

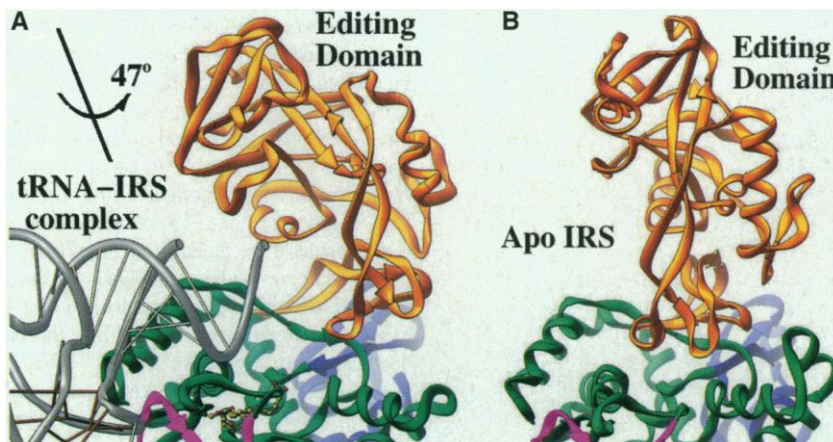


Fig. 3. Change in orientation of the editing domain (yellow) relative to the catalytic Rossmann fold domain (green) produced by the binding of tRNA (white). The Rossmann fold domains of the liganded and unliganded enzymes were oriented similarly by least-squares superposition of the α -carbon atoms. (A) A cleft lies between the Mupirocin (ball and stick representation) and the expected position of the editing active site. The direction of the axis about which the editing domain rotates by 47° in going to the ligand-free form is shown. (B) The editing domain in the apo IleRS (6) overlaps the tRNA binding site.

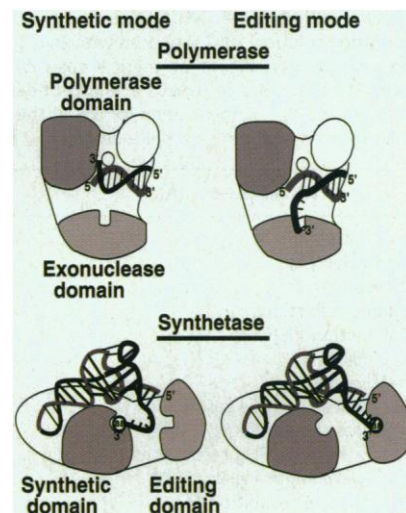


Fig. 4. Schematic cartoon comparing editing in DNA synthesis to editing in aminoacylation. In the synthetic mode of DNA replication, the 3' end of the double-stranded DNA lies in the polymerase active site marked by a small circle between the fingers and thumb. In the editing mode, a single-stranded primer strand lies in the 3' exonuclease active site (pocket), where nucleotides are removed. Similarly, in the synthetic mode of aminoacyl transfer, the acceptor strand of the tRNA forms a hairpinned conformation to pack against residues of the Rossmann fold; in the editing mode, the tRNA adopts the extended stacked conformation to place the amino acid in the editing domain (pocket).

the D-loop that must be the tRNA^{lle} sequence (7). Because this D-loop sequence does not interact with the protein in this crystalline complex, the explanation for the dependence of editing on this sequence is not immediately apparent. Either the protein undergoes a major conformational change, perhaps bringing the editing domain in contact with the D-loop sequence, or the influence of this sequence is expressed through the tRNA structure. In either case, the misacylated substrates would have to travel between the two active sites.

A similar dynamic competition between the synthetic and editing sites is also used in DNA polymerase editing (17). In Klenow fragment of *Escherichia coli* DNA polymerase I, double-stranded DNA binds to the polymerase active site and a melted out single-stranded primer terminus binds to the editing active site (17). The shuttling of the DNA substrate between the two active sites of Klenow fragment can occur by dissociation from one site and reassociation with the other or by processive sliding (18). We propose that the editing of both misincorporated nucleotides by DNA polymerase and misaminoacylation of tRNA or ATP by IleRS may proceed by analogous shuttle mechanisms (Fig. 4).

References and Notes

1. L. Pauling, in *Festschrift für Prof. Dr. Arthur Stoll*, Birkhauser Verlag, Basel (1958), p. 597.
2. R. B. Lofffield, *Biochem. J.* **89**, 82 (1963).
3. A. N. Baldwin and P. Berg, *J. Biol. Chem.* **241**, 839 (1966).
4. A. R. Fersht and C. Dingwall, *Biochemistry* **18**, 1238 (1979).
5. L. Lin, S. P. Hale, P. Schimmel, *Nature* **384**, 33 (1996).
6. O. Nureki et al., *Science* **280**, 578 (1998).
7. S. P. Hale, D. S. Auld, E. Schmidt, *ibid.* **276**, 1250 (1997).
8. A. R. Fersht, *ibid.* **280**, 541 (1998).
9. L. F. Silvis, J. Wang, T. A. Steitz, unpublished data.
10. V. R. Rath, L. F. Silvis, B. Beijer, *Structure* **6**, 439 (1998).
11. To position an aminoacyl-adenylate analogue (QSI) from the glutamyl-tRNA ternary complex (70) into the IleRS structure, we used the program O to superimpose α -carbon atoms from the Rossmann folds of the GlnRS and IleRS complexes; α -carbons that superimposed with a difference of less than 2.5 Å were used.
12. E. Schmidt and P. Schimmel, *Biochemistry* **34**, 11204 (1995).
13. F. Suddath et al., *Nature* **248**, 20 (1974).
14. M. A. Rould, J. J. Perona, D. Söll, *Science* **246**, 1135 (1989); J. J. Perona, M. A. Rould, T. A. Steitz, *Biochemistry* **32**, 8758 (1993).
15. To construct a model of the CCA end for the conformation required for amino acid transfer, we superimposed the phosphate backbone of the duplex acceptor stem of tRNA^{Gln} on that of tRNA^{lle} and the tRNA^{Gln} conformation used for a starting model (Fig. 2A); nucleotides 73 to 76 of the tRNA^{lle} were adjusted on the IleRS structure to prevent steric clashes and to correctly place the O2' of the terminal adenosine. To model build the disordered 3' terminal C75A76 of tRNA^{lle}, we superimposed the phosphate backbone of nucleotides 72 to 74 on A-form RNA, which was then used to extend the 3' tail by 2 nucleotides.
16. J. D. Heck and G. W. Hatfield, *J. Biol. Chem.* **263**, 868 (1988).
17. P. S. Freemont, J. M. Friedman, L. S. Beese, *Proc. Natl. Acad. Sci. U.S.A.* **85**, 8924 (1988); L. S. Beese and T. A. Steitz, *EMBO J.* **10**, 25 (1991); C. M. Joyce and T. A. Steitz, *Annu. Rev. Biochem.* **63**, 777 (1994).

18. C. M. Joyce, *J. Biol. Chem.* **264**, 10858 (1989).
19. J. Wang, unpublished data.
20. CCP4: Collaborative Computational Project No. 4, *Acta Crystallogr. D* **50**, 760 (1994).
21. J. P. Abrahams and A. G. W. Leslie, *ibid.* **52**, 30 (1996).
22. M. A. Rould, J. J. Perona, T. A. Steitz, *Acta Crystallogr. A* **48**, 751 (1992).
23. T. A. Jones and M. Kjeldgaard, *O Manual* (Uppsala, Sweden, 1994).
24. A. F. Chalker, J. M. Ward, A. P. Fosberry, *Gene* **141**, 103 (1994).
25. In preparation for crystallization, we dialyzed IleRS into 20 mM Bicine (pH 8.0), 50 mM KCl, 5 mM MgCl₂, 2 mM 2-mercaptoethanol, 1 mM ZnCl₂ and then concentrated it to 20 mg/ml in a Centricon 15 (Amicon). We then folded the tRNA transcript by dissolving a lyophilized pellet in 10 mM sodium cacodylate (pH 6.0), 5 mM MgCl₂ at a concentration of 5 mg/ml, heating at 60°C for 5 min, and then slow-cooling to 25°C for an hour. We then lyophilized the tRNA and redissolved to a concentration of 20 mg/ml with 40 mM sodium cacodylate (pH 6.0) and 20 mM MgCl₂. The complex of 50 μ M IleRS, 50 μ M tRNA, and 1 mM Mupirocin was mixed with the well solution at a well:complex ratio of 3:1 (v/v). The well solution contained 12% PEG 6K, 0.3 M KCl, 100 mM sodium cacodylate (pH 6.3), 100 mM MgSO₄, 2 mM ZnCl₂, and 0.1% β -octyl glucopyranoside. The drops were streak-seeded without prior equilibration and then equilibrated at 20°C by the hanging-drop method. Crystals were frozen by replacing the mother liquor with a cryoprotectant containing the well solution with the addition of PEG 6K to a final concentration of 20% (w/v) and ethylene glycol to a final concentration of 15% (v/v) and then flash-freezing in liquid propane.
26. O. Nureki et al., *J. Mol. Biol.* **236**, 710 (1994).
27. Derivatives were phased in MLPhare with CCP4 by an innovative method called permuting the native/derivative (19). In this procedure, data collected at each of the MAD wavelengths were considered the "native" in four parallel MIR refinements, and then phases from all four refinements were combined by their Hendrickson-Lattmann coefficients in SigmaA (20). We measured phase improvement by the objective criterion of monitoring the height of a difference Fourier peak of an independent derivative for which there was a clear difference Patterson peak. Using the selenium derived phases, we identified additional sites in other derivatives. The MAD and MIR phase sets from all derivatives were combined by using SigmaA weighting and the resultant map was modified in Solomon (21). In a second round, the heavy atom parameters were independently refined by using density-modified external phases (22) and all phase sets were combined again. In the large cell, we traced the course of the backbone of the entire protein by using experimental maps with the exception of a region between residues 205 and 390 in the editing (CP1) domain and the last 4 nucleotides of the tRNA. In the small cell, the entire protein is ordered with the exception of the COOH-terminal, Zn-binding domain, a region between residues 205 and 390 in the editing domain, and the last 2 nucleotides of the tRNA (Fig. 1B). Improvement in the phases was monitored by an increase in the real space correlation coefficient in O (23). After this manuscript was submitted, the coordinates of *T. thermophilus* IleRS (6) became available and we used them to improve and extend our incomplete model of the editing domain.
28. T. C. Terwilliger, *Acta Crystallogr. D* **50**, 17 (1994).
29. A. M. Friedman, T. O. Fischmann, Y. Shamoo, American Crystallographic Association Annual Meeting, Atlanta, GA, abstract TRN07 (1994).
30. P. D. Adams, N. S. Pannu, R. J. Read, *Proc. Natl. Acad. Sci. U.S.A.* **94**, 5018 (1997).
31. Supported by National Institutes of Health (NIH) grant GM22778. We thank S. Abdel-Meguid at Smith-Kline Beecham for providing initial supplies of IleRS, Mupirocin, and the clone that overproduces IleRS; L. Rice and S. Smerdon for cloning the tRNA^{lle} gene used for tRNA transcription; T. Terwilliger, R. Sweet, L. Berman, and C. Ogata for access to beamlines at Brookhaven National Laboratory; and D. Thiel for Beamlines at Cornell High Energy Synchrotron Source. We thank C. Correll, S. Kamtekar, G. Cheetham, C. Brautigam, J. Ippolito, P. Klosterman, N. Ban, S. Szep, V. Korada, and J. Pata for help collecting data. Coordinates of the IleRS:tRNA Mupirocin complex and the structure factor amplitudes have been deposited in the Protein Data Bank (accession codes PDB 1QU2 and PDB 1QU3) and in Research Collaborating for Structural Bioinformatics at the University of New Jersey, Rutgers (RCSB009293).

30 December 1998; accepted 8 July 1999

Quaternary Structure of the Insulin-Insulin Receptor Complex

Robert Z.-T. Luo,¹ Daniel R. Beniac,² Allan Fernandes,² Cecil C. Yip,^{1*} F. P. Ottensmeyer^{2*}

The three-dimensional (3D) structure of the intrinsically dimeric insulin receptor bound to its ligand, insulin, was determined by electron cryomicroscopy. Gold-labeled insulin served to locate the insulin-binding domain. The 3D structure was then fitted with available known high-resolution domain substructures to obtain a detailed contiguous model for this heterotetrameric transmembrane receptor. The 3D reconstruction indicates that the two α subunits jointly participate in insulin binding and that the kinase domains in the two β subunits are in a juxtaposition that permits autophosphorylation of tyrosine residues in the first step of insulin receptor activation.

The cellular receptor for the hormone insulin is a transmembrane receptor tyrosine kinase (TK) that is a disulfide-linked dimer. The 480-kD insulin receptor (IR) is composed of two heterodimers, each of which contains an α and β chain (1, 2). Binding of insulin to the extracel-

lular domain of the intrinsically dimeric IR results in autophosphorylation of specific tyrosines in the IR cytoplasmic domain and the initiation of an intracellular signal transduction cascade (3). However, the structural basis for IR activation by insulin has not been elucidated